Smart Battery Management Systems: Internal State Estimation of Lithium-ion Batteries Under Thermal Faults

Geetika Vennam, Avimanyu Sahoo, and Saima Alam

Email: *avimanyu.sahoo@uah.edu*

THE UNIVERSITY OF ALABAMA IN HUNTSVILLE

November 15, 2023

Overview

Introduction

- **Vehicle recalls:**
  - GM Chevrolet Bolt recall: high-voltage battery pack catching fire
  - BMW and Ford recalls: battery fires, overheating, or failures.
  - Chrysler Pacifica Plug-in Hybrid minivans recall: investigating 12 fires.

Chevy bolt on fire [1]

Cell Degradation Mechanism

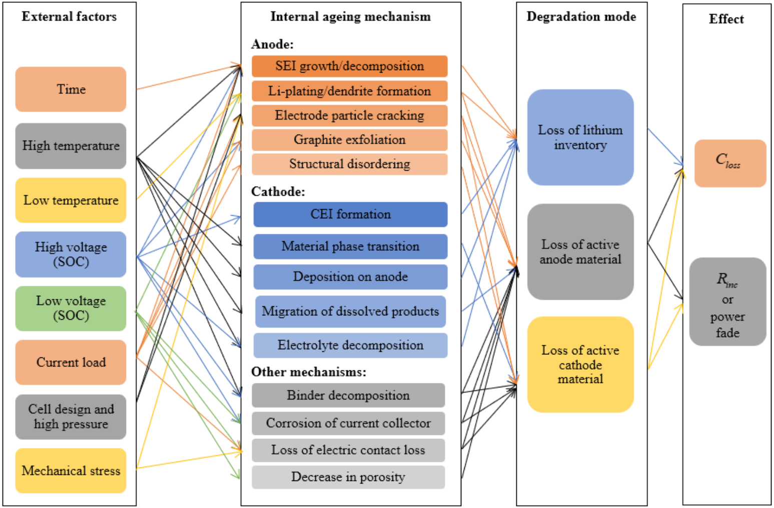

* Vennam, G., A. Sahoo, and S. Ahmed. "A survey on lithium-ion battery internal and external degradation modeling and state of health estimation." Journal of Energy Storage 52 (2022): 104720.

Need

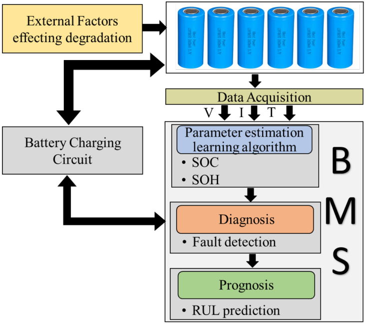

1. Advanced battery models which accounts for SOH.
2. Algorithms which can simultaneously estimate SOC, SOH along with internal parameters.
3. Development of fault detection schemes to detect faults at an incipient stage.
4. Development of estimation scheme that can estimate the internal parameter under faults

Current State-of-the-Art: Modeling

- Electro-thermal model [2]
  - Monitor internal temperature.
  - Study the thermal effects on battery's parameters.
- Electro-thermal-aging models [3, 4, 5, 6].

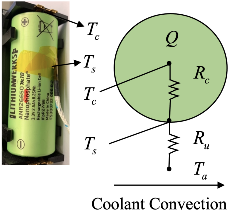

Fig. 1: Thermal model of LFP cell

2RC ECM [3]

$$\frac{dSOC}{dt} = \frac{-I}{C_{use}}$$
$$\frac{dV_{c_{p1}}}{dt} = \frac{-V_{c_{p1}}}{R_{p1}C_{p1}} + \frac{I}{C_{p1}}$$
$$\frac{dV_{c_{p2}}}{dt} = \frac{-V_{c_{p2}}}{R_{p2}C_{p2}} + \frac{I}{C_{p2}} +$$
$$V_t = V_{OC}(SOC) - V_{c_{p1}} - V_{c_{p2}} - R_0 I \quad (1)$$

Thermal model [7]

$$\dot{T}_c = \frac{T_s - T_c}{R_c C_c} + \frac{Q(t)}{C_c}$$
$$\dot{T}_s = \frac{T_a - T_s}{R_u C_s} - \frac{T_s - T_c}{R_c C_s} + \quad (2)$$

Capacity fade model [8]

$$C_{loss} = M(c)\, e^{\frac{31700 - 370.3 C_{rate}}{R_g T_c}} (Ah)^z \quad (3)$$

Current State-of-the-Art

Limitations:

- Constant parameter models [3, 9].
- ECM employed is not coupled with the capacity fade dynamics.
  - Effects of capacity fade (SOH) on SOC and, in turn, the ECM parameters and the terminal voltage are not reflected.

SOH-inclusive Model of LIB

- ECM is presented by integrating the capacity fade dynamics.
- Alternatively ECM parameters can be represented to vary with temperature, aging, C_{rate} and capacity loss.

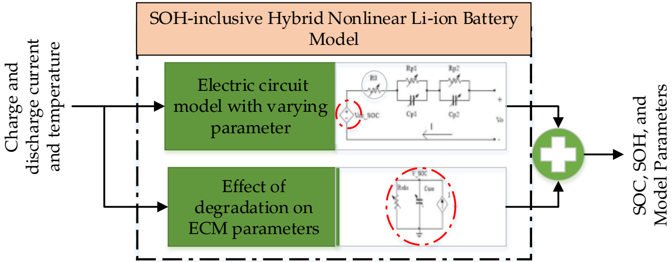

SOH-inclusive Model of LIB

- SOH-coupled model of LIB a) ECM, b) thermal model, c) capacity fade model.

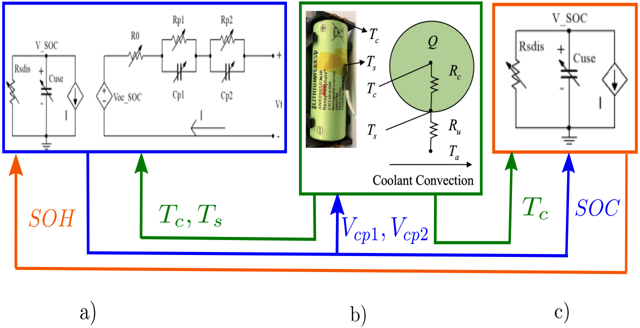

SOH-coupled model

ECM

$$
\begin{aligned}
\frac{dSOC}{dt} &= \frac{-I}{C_{use} * SOH(t)} \\
\frac{dV_{c_{p1}}}{dt} &= \frac{-V_{c_{p1}}}{R'_{p1}C'_{p1}} + \frac{I}{C'_{p1}} \\
\frac{dV_{c_{p2}}}{dt} &= \frac{-V_{c_{p2}}}{R'_{p2}C'_{p2}} + \frac{I}{C'_{p2}} \qquad + \\
V_t &= V_{OC}(SOC) - V_{c_{p1}} - V_{c_{p2}} - R'_0 I
\end{aligned}
\tag{4}
$$

Thermal Model

$$
\begin{aligned}
\dot{T}_c &= \frac{T_s - T_c}{R_c C_c} + \frac{Q(t)}{C_c} \\
\dot{T}_s &= \frac{T_a - T_s}{R_u C_s} - \frac{T_s - T_c}{R_c C_s} \qquad +
\end{aligned}
\tag{5}
$$

Capacity Fade Model

$$
\begin{aligned}
C_{loss} &= (\alpha SOC + \beta) e^{\frac{E_a + \eta C_{rate}}{R_g T_c}} (Ah)^z \\
\dot{SOH}(t) &= -\frac{|I(t)|}{2N(C_{rate}, T_c) C_{use}}
\end{aligned}
\tag{6}
$$

$R'_0 = R_0(T_m)$, $R'_{p1} = R_{p1}(SOC, T_m)$, $R'_{p2} = R_{p2}(SOC, T_m)$, $C'_{p1} = C_{p1}(SOC, T_m)$, $C'_{p2} = R_{p2}(SOC, T_m)$, $Q(t)$ is the heat generation term.

SOH-coupled Model Validation

- A 10A CC-CV input current is used to observe degradation over life
- SOC for the first charge-discharge cycle
- SOC for a time window at approximate mid-life
- SOH decay for end of life cycle

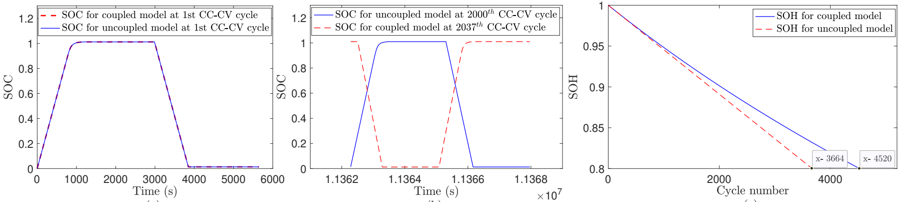

(a) (b) (c)

SOH-coupled Model Validation

- Comparison results with experimental validation results in [10].
- Proposed SOH-coupled model number of cycles is closer to the experimental results [10].
- Proposed SOH-coupled model more accurately represents the actual cell dynamics and number of cycles of operation.

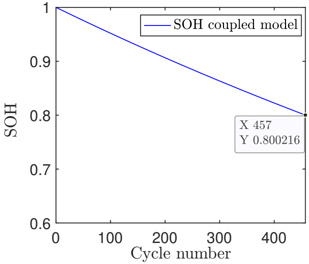

(a)

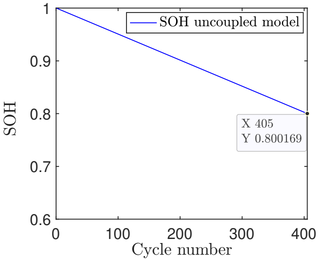

(b)

SOH decay $(4.17C_{rate}, 65°C)$ for coupled a) and b) uncoupled model.

Experimental Setup

- Maccor test equipment

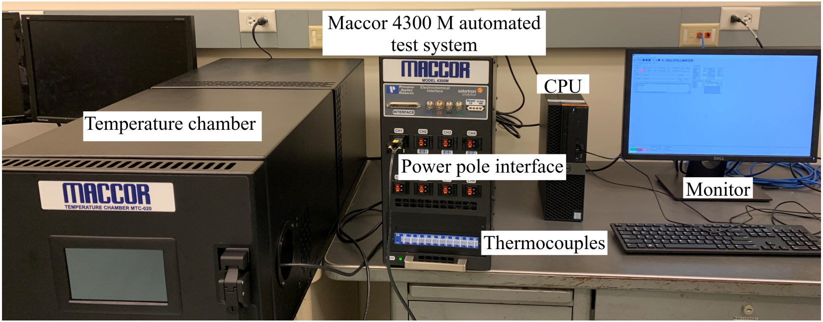

Experimental Setup

- A123 2.5 Ah 26650 $LiFePO_4$ cell is selected for experiments
- The capacity of the cell is measured experimentally by cycling the battery at low rate (C/20) and found to be 2.4Ah.
- The $V_{oc}(SOC)$ curve is obtained from OCV-SOC test
- Identification of parameters using pulse charge/discharge test

OCV-SOC Test

1. Conduced the charge-discharge test to find the SOC-OCV curve.

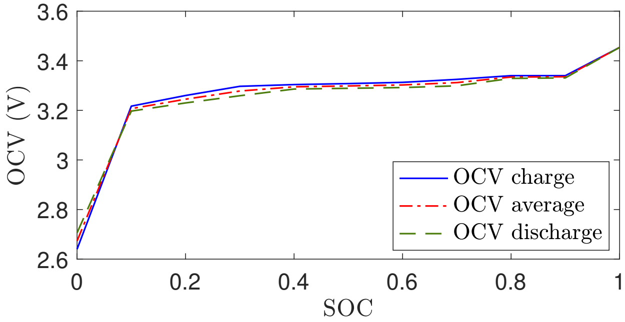

- Pulse charging and discharging test at different temperatures ($15°C$, $25°C$, $35°C$, $45°C$)

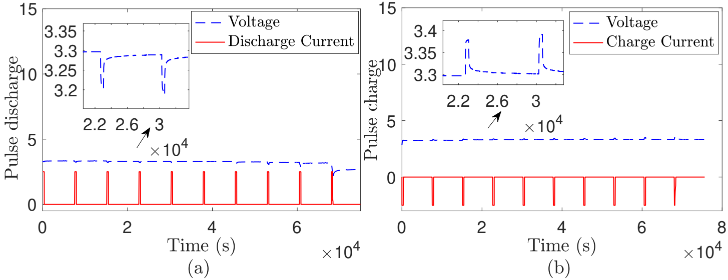

Experimental Results: A12326650 2.5Ah

- A drive cycle current profile used as an input.

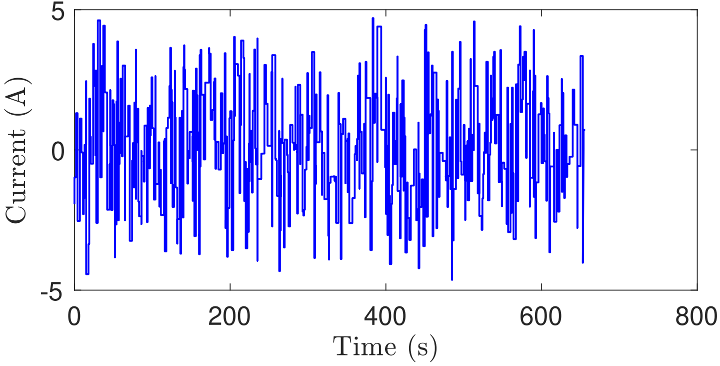

Experimental Validation of SOH-inclusive Model

- Output voltage RMSE: $0.0063V$
- Surface temperature RMSE: $0.0926°C$

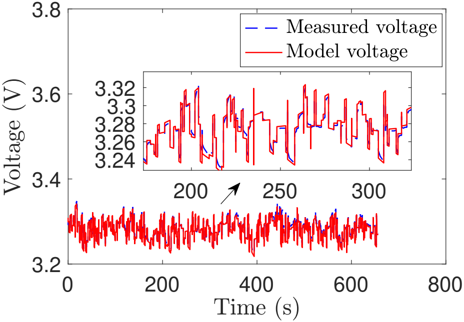

(a)

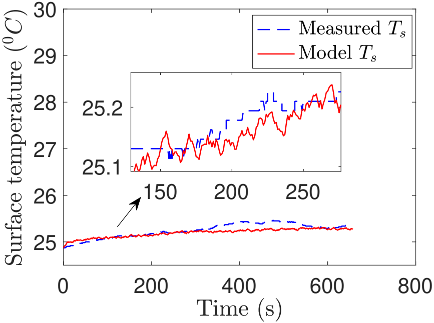

(b)

Fault Detection: Previous Works and Limitations

- Previous works:
  - Two state electro-thermal model [11, 12] to detect internal thermal faults using core and surface temperatures as residuals
  - Battery internal resistance estimator [12] to represent the changes in core temperature due to fault.
- Limitations:
  - ECM parameter (R_0) varies with SOH and other degradation inducing factors, such as T_c, C_{rate}, and DOD.
  - Thermal model parameters, such as C_c, C_s, T_a also change with battery aging.
  - Account for the changes in residuals due to the aging, change in operating conditions, and unmodeled dynamics (uncertainty) and eliminate false positives.

Fault Detection and Internal State Estimation Scheme

- Fault detection scheme for SOC, SOH and core temperature estimation during faults

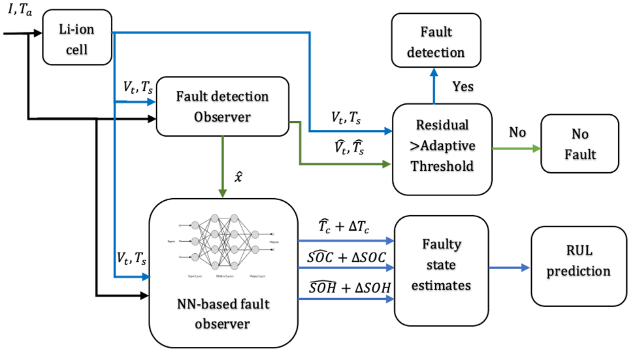

Fault Detection: Fault Mapping

Actual faults	Description of fault	Fault map
Fault 1	Convective cooling resistance fault (ΔR_u).	$\gamma_4 = 0$, $\gamma_5 \neq 0$, $\gamma_7 \neq 0$
Fault 2	Internal thermal resistance fault (ΔR_c).	$\gamma_4 \neq 0$, $\gamma_5 \neq 0$, $\gamma_7 \neq 0$
Fault 3	Thermal runaway fault	$\gamma_4 \neq 0$, $\gamma_5 = 0$, $\gamma_7 \neq 0$
Fault 4	Internal side reaction fault	$\gamma_4 \neq 0$, $\gamma_5 \neq 0$, $\gamma_7 \neq 0$

Fault Detection: Fault Detection Scheme

The state space model in with the above faults can be expressed as

$$\dot{x}_f = Kx_f + \Pi(x_f) + g(x_f)u + \Gamma(x_f, u) \tag{7}$$

where x_f are the faulty states of the model, the vector $\Gamma(x_f, u) = [0\ 0\ 0\ \gamma_4(t)\ \gamma_5(t)\ 0\ \gamma_7(t)\ 0]^T$ are the faults added to the dynamics of the battery.

- $\gamma_4(t)$ represents fault in core temperature dynamics.
- $\gamma_5(t)$ represents fault in surface temperature dynamics.
- $\gamma_7(t)$ represents fault in internal resistance dynamics.

Fault Detection Scheme

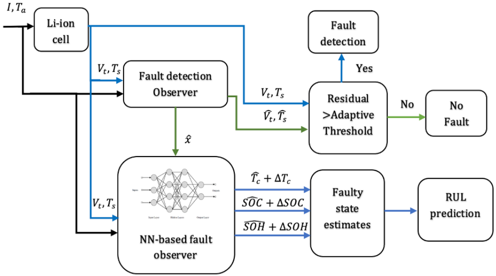

- SOH-integrated cell model

$$\begin{aligned} \dot{x} &= Kx + \Pi(x) + g(x)u \\ y &= Cx \end{aligned} \quad (8)$$

- The nonlinear observer can be represented by

$$\begin{aligned} \dot{\hat{x}} &= K\hat{x} + \Pi(\hat{x}) + g(\hat{x})u + L^T(y - \\ \hat{y} &= C\hat{x} \end{aligned} \quad (9)$$

Healthy observer desing

- A nonlinear observer is designed
- The observer used SOH-coupled model to accurately estimate the SOC, SOH, and internal resistance accurately

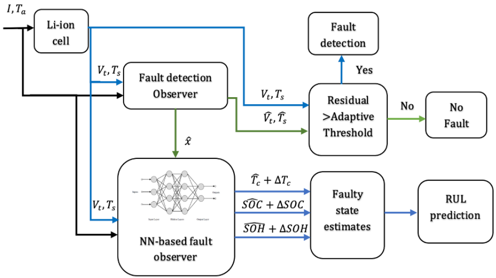

- Adaptive threshold

$$R_{es_{1th}} = \tilde{y}_1(0)e^{-\sigma_5 t} + \Psi_1, \text{ and}$$
$$R_{es_{2th}} = \tilde{y}_2(0)e^{-\sigma_8 t} + \Psi_2, \tag{10}$$

$$\dot{\Psi}_1 = -\sigma_5\Psi_1 + \eta_{5max},$$
$$\dot{\Psi}_2 = -\sigma_8\Psi_2 + \eta_{8max}. \tag{11}$$

Adaptive threshold for fault detection

- Change in model parameters due to health
- Modeling uncertainty
- An adaptive threshold is designed to account for the above

- **Only uncertainties and no-fault:** Output residuals and adaptive thresholds
- T_s RMSE: 0.0038, Voltage RMSE: 0.0033
- All the state estimation errors for SOH, SOC, R_0, T_C are within 1% band.

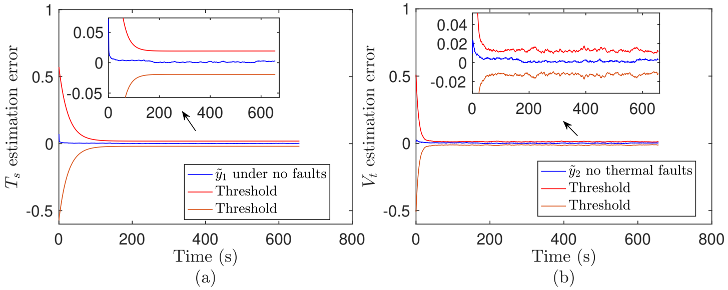

- A **convective cooling resistance** fault $0.4R_u$ is introduced to the system at $t = 206$ sec.
- The residual V_t and T_s exceeds the threshold value after $t = 206$ sec.

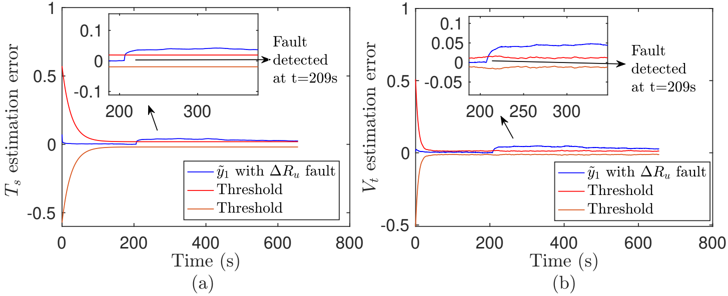

Internal State Estimation Under Fault

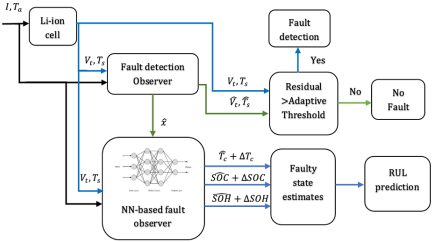

$$\dot{\check{x}} = K\check{x} + \Pi(\check{x}) + g(\check{x})u + \check{\theta}^T\sigma(\check{x}, u) + L^T C\tilde{x} \qquad (12)$$
$$\check{y} = C\check{x}$$

Neural network-based observer to learn faulty states

- The healthy observer and a neural network.
- The neural network kicks in once the fault is detected.

Estimation of faulty states

- The Major challenge is the limited available measurement
- The estimated healthy states, as a substitute for the states that are not measurable, are used in addition to the faulty measured output.
- The weight update law, developed based on stability analysis, can be represented by

NN Weight Update Law

$$\dot{\hat{\theta}} = -\sigma(\check{x}, u)\Xi^T \upsilon - \sigma(\check{x}, u)\sigma(\check{x}, u)^T \hat{\theta}\Upsilon \tag{13}$$

where $\upsilon, \Upsilon \in \mathbb{R}^{n\times n}$ are the learning gains and $\Xi = \bar{X} - \check{x}$, with

$$\bar{X} = [S\hat{O}C, \hat{V}_{cp1}, \hat{V}_{cp2}, \hat{T}_c, y_{1f}, S\hat{O}H, \hat{R}_0, y_{2f}]^T$$

Simulation Results

- NN weight $\hat{\theta}$ was initialized at random from a uniform distribution in the interval of $[0\ 0.001]$, $l = 20$.

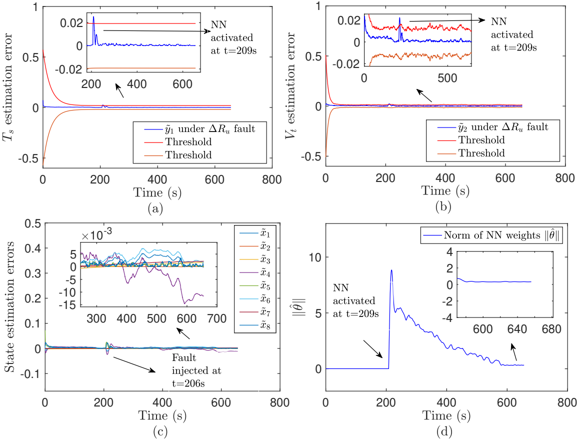

Simulation Results: Multiple Faults

- A convective cooling resistance $0.4R_u$, internal thermal resistance $0.2R_c$, and thermal runaway $0.02\mathrm{W}$ faults are injected at $t = 206$ sec
- The residual T_s and V_t exceeds the threshold value after $t = 206$ sec, respectively.

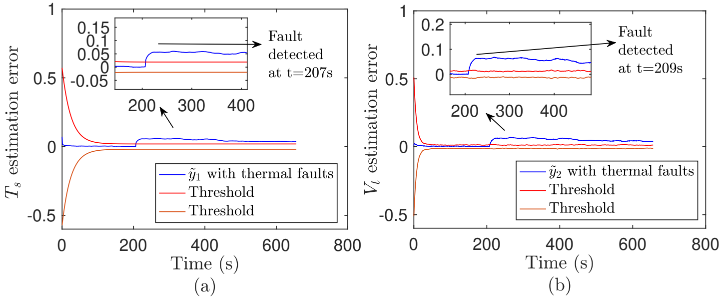

Simulation Results: Multiple Faults

- NN weight $\hat{\theta}$ was initialized at random from a uniform distribution in the interval of $[0\ 0.001]$, $l = 20$.

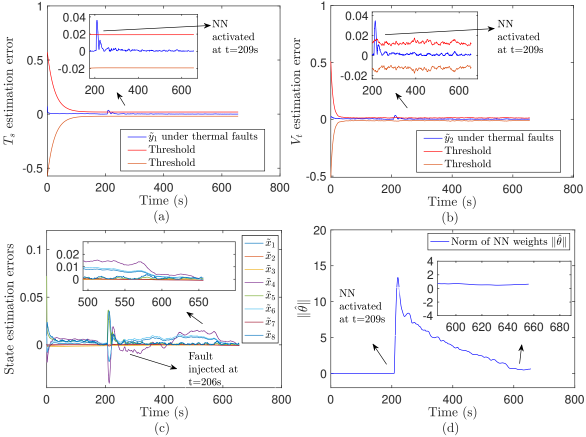

Conclusions

- We presented a SOH-integrated model and validated the experimentally
- Subsequently, we used the model for fault detection by developing a fault detection observer.
- We designed an adaptive threshold accounting for health degradation.
- NN-based fault detection scheme to detect thermal and also estimate the core temperature, SOC, and SOH during faults.

Current and Future Work

- Extend the cell model to a pack level with electrical and thermal interconnection
- Develop an identification scheme to estimate pack model parameters.
- Extend the learning capability to estimate spatial variables using spatiotemporal learning.

References I

[1] K. Gale, "Chevy bolt," 2020.
Last accessed 16 September 2017.

[2] X. Lin, H. E. Perez, S. Mohan, J. B. Siegel, A. G. Stefanopoulou, Y. Ding, and M. P. Castanier, "A lumped-parameter electro-thermal model for cylindrical batteries," *Journal of Power Sources*, vol. 257, pp. 1–11, 2014.

[3] H. E. Perez, X. Hu, S. Dey, and S. J. Moura, "Optimal charging of li-ion batteries with coupled electro-thermal-aging dynamics," *IEEE Transactions on Vehicular Technology*, vol. 66, no. 9, pp. 7761–7770, 2017.

[4] H. Pang, L. Guo, L. Wu, J. Jin, F. Zhang, and K. Liu, "A novel extended kalman filter-based battery internal and surface temperature estimation based on an improved electro-thermal model," *Journal of Energy Storage*, vol. 41, p. 102854, 2021.

[5] N. Guo, X. Zhang, Y. Zou, L. Guo, and G. Du, "Real-time predictive energy management of plug-in hybrid electric vehicles for coordination of fuel economy and battery degradation," *Energy*, vol. 214, p. 119070, 2021.

[6] K. Liu, C. Zou, K. Li, and T. Wik, "Charging pattern optimization for lithium-ion batteries with an electrothermal-aging model," *IEEE Transactions on Industrial Informatics*, vol. 14, no. 12, pp. 5463–5474, 2018.

[7] H. E. Perez, J. B. Siegel, X. Lin, A. G. Stefanopoulou, Y. Ding, and M. P. Castanier, "Parameterization and validation of an integrated electro-thermal cylindrical lfp battery model," in *Dynamic Systems and Control Conference*, vol. 45318, pp. 41–50, American Society of Mechanical Engineers, 2012.

[8] G. Suri and S. Onori, "A control-oriented cycle-life model for hybrid electric vehicle lithium-ion batteries," *Energy*, vol. 96, pp. 644–653, 2016.

[9] W. Li, L. Liang, W. Liu, and X. Wu, "State of charge estimation of lithium-ion batteries using a discrete-time nonlinear observer," *IEEE Trans. Ind. Electron*, vol. 64, no. 11, pp. 8557–8565, 2017.

[10] NASA, "Development of battery packs for space applications."

References II

[11] S. Dey, Z. A. Biron, S. Tatipamula, N. Das, S. Mohon, B. Ayalew, and P. Pisu, "Model-based real-time thermal fault diagnosis of lithium-ion batteries," *Control Engineering Practice*, vol. 56, pp. 37–48, 2016.

[12] J. Wei, G. Dong, and Z. Chen, "Lyapunov-based thermal fault diagnosis of cylindrical lithium-ion batteries," *IEEE Transactions on Industrial Electronics*, vol. 67, no. 6, pp. 4670–4679, 2019.

Questions?